DØ Note 5464-Conf

Search for the Associated Production of Chargino and Neutralino in Final States with Two Electrons and an Additional Lepton

The DØ Collaboration
URL: http://www-d0.fnal.gov
(Dated: April 7, 2008)

A search has been performed for the trilepton decay signature from the associated production of the lightest chargino and the next-to-lightest neutralino in leptonic channels with at least two electrons in the context of minimal Supersymmetry. The search uses data collected with the DØ detector during Run IIb at the Fermilab Tevatron $p\bar{p}$ collider at a center-of-mass energy of 1.96 TeV corresponding to an integrated luminosity of around 590 pb^{-1}. No candidates have been found, with an expected background of 1.0 ± 0.3 events. In combination with results in four other trilepton search channels based on approximately 1 $\text{fb}^{-1}$of Run IIa data, new stringent limits on the associated production of charginos and neutralinos have been set.

Preliminary Results for Summer 2007 Conferences

I. INTRODUCTION

Supersymmetry (SUSY) [1] postulates a symmetry between bosonic and fermionic degrees of freedom and predicts the existence of a supersymmetric partner for each standard model particle. The present analysis searches for the associated production of the charged (charginos) and neutral (neutralinos) partners of the electroweak gauge and Higgs bosons in final states with two electrons, a third lepton and large missing transverse energy. The analysis is based on the Minimal Supersymmetric extension of the Standard Model (MSSM) with R-parity conservation [1]. The model predicts the associated production of the lightest chargino ($\tilde{\chi}_1^{\pm}$) and the next-to-lightest neutralino ($\tilde{\chi}_2^0$) at $p\bar{p}$ colliders with subsequent decays into fermions and the the lightest supersymmetric particle, $\tilde{\chi}_1^0$, (the LSP), [2]. This note describes the search for purely leptonic decay modes optimized for the process $p\bar{p} \rightarrow \tilde{\chi}_1^{\pm}\tilde{\chi}_2^0 + X \rightarrow \ell ee\nu\tilde{\chi}_1^0\tilde{\chi}_1^0 + X$. The results are interpreted using a model motivated by the more specific minimal supergravity with chargino and neutralino masses mainly following the relation $m_{\tilde{\chi}_1^{\pm}} \approx m_{\tilde{\chi}_2^0} \approx 2m_{\tilde{\chi}_1^0}$. The chargino/neutralino decay mode depends on the mass relation to the scalar partners of the charged leptons (sleptons). The points in mSUGRA parameter space considered here are characterized by slepton masses close to the chargino/neutralino masses, which lead to an enhanced leptonic branching fraction. The present note focuses on 3-body decays via off-shell gauge bosons and sleptons (see Fig. 1), which are enhanced with respect to the cascade decay via sleptons for slepton masses comparable or larger than the chargino/neutralino masses. The result is interpreted in a scenario without slepton mixing and with degenerate $\tilde{e}_R$, $\tilde{\mu}_R$ and $\tilde{\tau}_R$ masses. Searches for supersymmetric particles have been performed in e^+e^- collisions at LEP [3] and in $p\bar{p}$ collisions at DØ [4, 5] and CDF [6]. No evidence for these particles has been found so far. LSP masses below 40 GeV are excluded in MSSM models with GUT relations by the LEP experiments. In mSUGRA, the LSP lower mass limit is found at 50-60 GeV [3]. For large slepton/sneutrino masses, chargino masses are excluded nearly up to the kinematic production threshold of 103 GeV by direct searches at LEP [3]. Higgs searches at LEP yield indirect sensivity also for the mass region beyond the chargino production threshold.

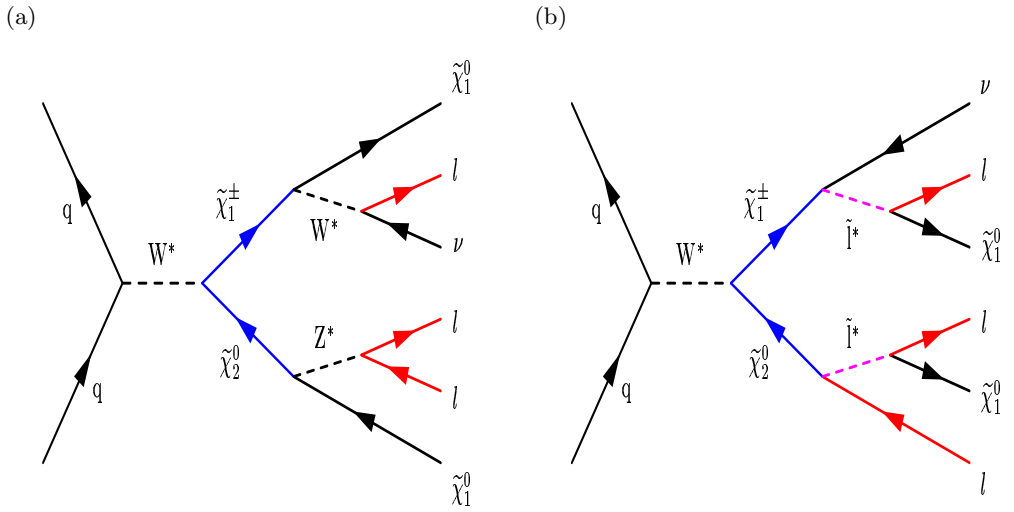

FIG. 1: Main production and decay modes for the signal points considered in the present analysis.

II. DATA AND MC SAMPLES

The analysis is based on data collected from June 2006 to April 2007 by the DØ detector [7] at the Fermilab Tevatron $p\bar{p}$ collider at a center-of-mass energy of 1.96 TeV and corresponds to an integrated luminosity of 588 pb^{-1}. The luminosity is determined by normalizing MC to data around the $Z \rightarrow ee$ peak at preselection level, using the NNLO cross section of 241.6 pb. The $Z/\gamma \rightarrow ee$ cross section is calculated with CTEQ6.1M PDFs as $\sigma(Z/\gamma \rightarrow ee) = \sigma_{LO} \times K_{QCD}(Q^2)$, with the LO cross section calculated by PYTHIA LO PDF and the K factor K_{QCD} at NNLO with NLO PDF, calculated according to [8, 9] as a function of the momentum transfer, Q^2. All simulated signal and standard model processes are generated using PYTHIA 6.319 [10] and processed through the full detector simulation. Signal parameter combinations have been generated for $\tan\beta = 3$ (see below) and chargino masses in the range of 115-150 GeV using the Les Houches Accords, (LHA) [11]. See Table I. Three reference points were chosen with

low, medium and high $\tilde{\chi}^{\pm}$ mass within this mass range. The symbols in Table I are: The common fermion mass at GUT scale, $m_{1/2}$, the common scalar mass at GUT scale, m_0, the ratio of vacuum expectation values of the two Higgs fields, tanβ, the trilinear coupling A_0 and the Higgs(ino) mass parameter, μ. The total cross section $\sigma \times \mathrm{BF}(\mathrm{p\bar{p}} \to \tilde{\chi}_1^{\pm}\tilde{\chi}_2^0 \to 3\ell)$ varies between 0.03 and 0.2 pb. A detailed description of the generated reference points is given in Table I. Major background sources are $\mathrm{Z}/\gamma \to \mathrm{ee}$, $\mathrm{W}+\gamma \to \mathrm{e}\nu+\gamma$, and $\mathrm{WW} \to \mathrm{ee}\nu\nu$. Multijet background from QCD production is determined directly from data. For this, a sample dominated by multijet background has been defined that are identical to the search sample except for an inverted electron identification requirement. The resulting sample corresponds to dijet events with jets that are broader than the jets actually preselected in the analysis. To correct this sample for trigger dependencies, the subsample of the data with like-sign electrons is used. The like-sign sample is dominated by QCD events at preselection level, but cannot be used in advanced stages of the analysis, since the signal is partly like sign. All standard selection cuts are applied to the QCD sample with inverted electron identification requirements, except cuts that strongly correlate with the reversed cut. For these cuts, the rejection is estimated from the like-sign sample. The QCD sample is normalized at an early stage of the selection in the low mass region. The trigger efficiency is taken into account by comparing the p_T distribution of the leading electron in Drell-Yan Z/γ^* events in data and MC.

name	$\tilde{\chi}^{\pm}$-mass (GeV)	$\tilde{\chi}_2^0$-mass (GeV)	$\tilde{\chi}_1^0$ mass (GeV)	m_0 (GeV)	$m_{1/2}$ (GeV)	$m_{\tilde{l_R}}$ (GeV)	$\sigma \times BR[pb]$
LHA.244.324	150	152	82	121	221	153	0.0366
LHA.131.232	125	127	69	98	192	129	0.123
LHA. 87.194	115	118	63	88	182	119	0.1984

TABLE I: SUSY parameters for three reference signal points. All points have tan$\beta = 3$, $A_0 = 0$, $\mu > 0$.

III. EVENT SELECTION

The selection procedure is summarized in Table II. It will be justified and described in more detail in the following. The selection requires two electrons with $p_{\mathrm{T}} > 8, 12$ GeV, with high electromagnetic energy fraction and passing energy isolation cuts. They are required to match in η and ϕ with a reconstructed track. An electron likelihood variable [12] based on tracking and calorimeter quantities is used to further enhance the purity of the electron sample. Both electrons must stem from the primary vertex and be reconstructed in detector pseudorapidity $|\eta_{\mathrm{det}}| < 3.0$ with at least one electron in the central region ($|\eta_{\mathrm{det}}| < 1.1$). To reduce the background from photon conversions, at least one hit in the silicon tracking detector (SMT) is required for the next-to-leading electron. This requirement is replaced by a tightened likelihood cut for events with a vertex outside the SMT acceptance.

TABLE II: Summary of the event selection criteria

(1) Preselection	$p_{\mathrm{T}} > 8\,\mathrm{GeV}, 12\,\mathrm{GeV}$ electrons high electron likelihood electrons from primary vertex at least one electron in the central calorimeter at least 1 Hit in the inner SMT for $\mid z_{\mathrm{PV}} \mid < 35$cm likelihood tightened for $\mid z_{\mathrm{PV}} \mid > 35$cm
(2) Anti $\mathrm{Z}/\gamma^* \to \mathrm{ee}$	$18\,\mathrm{GeV} < \mathrm{inv.\,mass} < 60\,\mathrm{GeV}$ $\Delta\phi(\mathrm{e},\mathrm{e}) < 2.9$ rad
(3) Anti $t\bar{t}$	$H_T < 80\,\mathrm{GeV}$
(4) Isolated Track	$p_T^{\ell 3} > 4.0\,\mathrm{GeV}$ isolation $\Sigma p_T < 1$ GeV, $E_{iso} < 3$ GeV $E_{iso} < 0.6 * \sqrt{p_T^{l3}}$
(5) $\not\!\!E_{\mathrm{T}}$ related	$\not\!\!E_{\mathrm{T}} > 22\,\mathrm{GeV}$ transverse mass (e+$\not\!\!E_{\mathrm{T}}$) $> 20\,\mathrm{GeV}$ Sig ($\not\!\!E_{\mathrm{T}}$) > 8.0
(6) Anti-W track	$p_T^{\ell 3} > 7\,\mathrm{GeV}$ if $M_T > 65$ GeV
(7) Anti-Z II	M(e, $p_T^{\ell 3}$) < 60 GeV or 120 GeV $<$ M(e, $p_T^{\ell 3}$) if track outside acceptance of calorimeter
(8) Tr$\times\not\!\!E_{\mathrm{T}}$	$\not\!\!E_{\mathrm{T}} \times \mathrm{p}_{\mathrm{T}}^{\ell 3} > 220$ GeV^2

Figure 2a shows the distribution in data, background and signal of the invariant dielectron mass at this stage of the selection. This stage is referred to as preselection stage. Most of the $Z/\gamma^* \to ee$ events are rejected by requiring the invariant dielectron mass to be in the range 18 GeV <M(ee) < 60 GeV. A large fraction of remaining back-to-back $Z/\gamma^* \to ee$ is reduced by requiring the opening angle between the leptons to be less than 2.9. The $t\bar{t}$ contribution is reduced by requiring H_T to be lower than 80 GeV. H_T is defined as the scalar sum of the transverse momenta of all jets in the event.

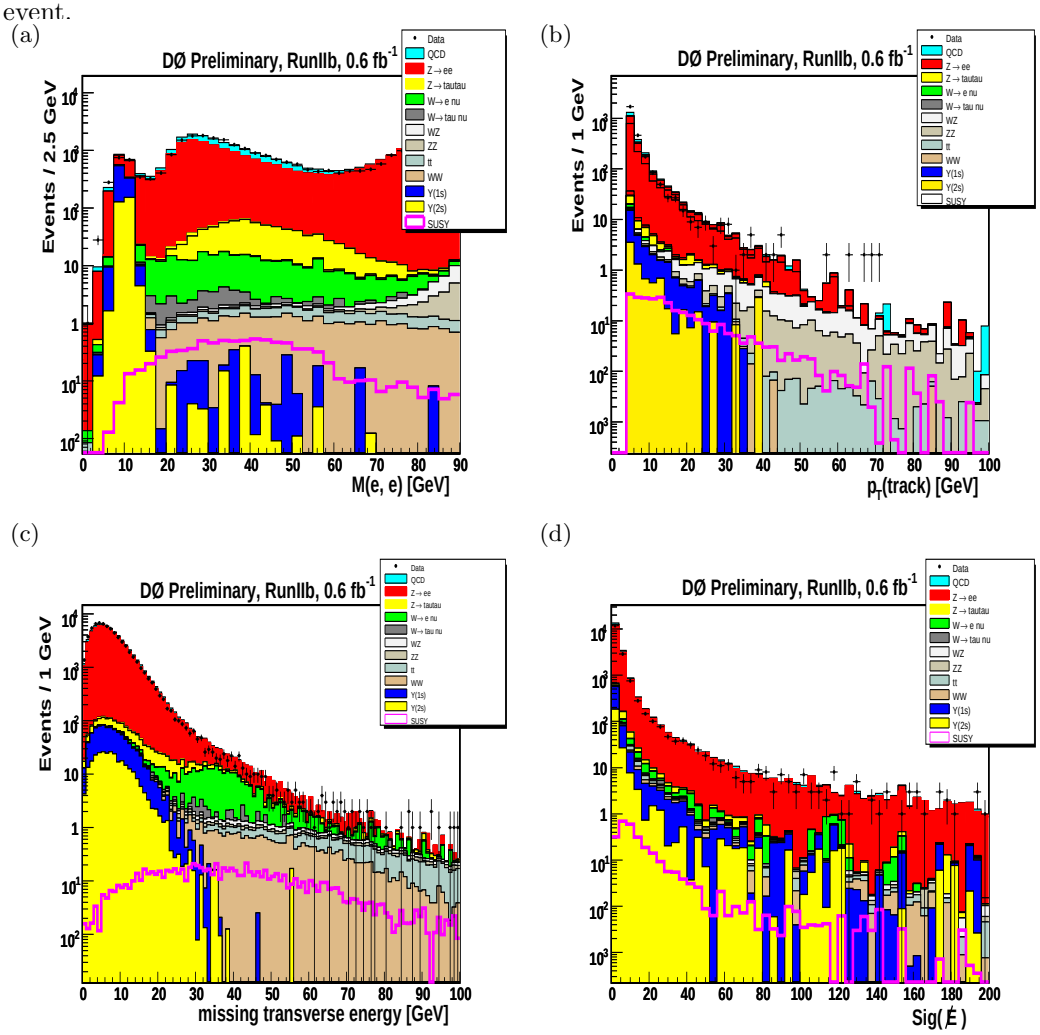

FIG. 2: Distribution of (a) the invariant dielectron mass at preselection level (b) the isolated track transverse momentum, $p_T^{\ell 3}$, at preselection level (c) the missing transverse energy, $\not\!\!E_{\rm T}$, at preselection level and (d) the scaled missing transverse energy, Sig($\not\!\!E_{\rm T}$), at preselection level for data (points with error bars), background simulation (histograms, complemented with the QCD expectation) and signal expectation for point LHA.131.232 (empty histogram).

The background at this stage consists mostly of $Z/\gamma^* \to ee$, $W \to e\nu$, and QCD events, and is significantly reduced by requiring an additional isolated track, well separated from the two electron candidates ($\Delta R = \sqrt{(\Delta\eta)^2 + (\Delta\phi)^2} > 0.4$) and also stemming from the primary vertex. To ensure a good p_T measurement also for forward tracks, either at least 17 hits in the tracking systems where at least one is in the fiber tracker or at least 14 hits in the fiber tracker are required. Tracks in jets are typically very close to other low-p_T particles, as opposed to the signal where the third track is expected to be isolated. Isolation is ensured by requiring the activity in a hollow cone $0.1 < \Delta R < 0.4$ around the track to be small. The cone is chosen to be hollow to also be efficient from tracks from τ decays, since all tau decay modes (leptonic, hadronic (1 prong), hadronic (3 prong)) either produce only 1 track or a set of tracks in a very narrow cone. Track isolation is done in two steps. First the p_T sum of other reconstructed tracks in the hollow cone is required to be less than 1 GeV. Then the calorimeter energy deposition in a hollow cone of $0.2 < \Delta R < 0.4$ is required to be less than 3 GeV and $\frac{\Sigma E_T}{GeV} < 60\% \sqrt{\frac{p_T^{\ell 3}}{GeV}}$ where $p_T^{\ell 3}$ denotes the p_T of the isolated track and ΣE_T is the scalar sum of the transverse energy in the electromagnetic and the fine hadronic cells. Figure 2b shows the $p_T^{\ell 3}$

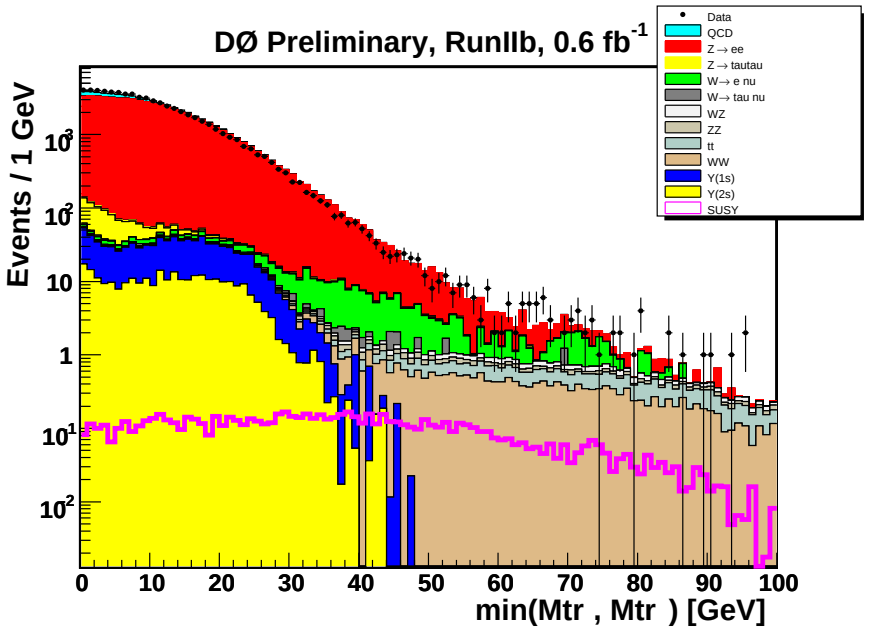

FIG. 3: Distribution of the minimum transverse mass at preselection level in data (points with error bars), background simulation (histograms, complemented with the QCD expectation) and signal expectation for SUSY point LHA.131.232 [11].

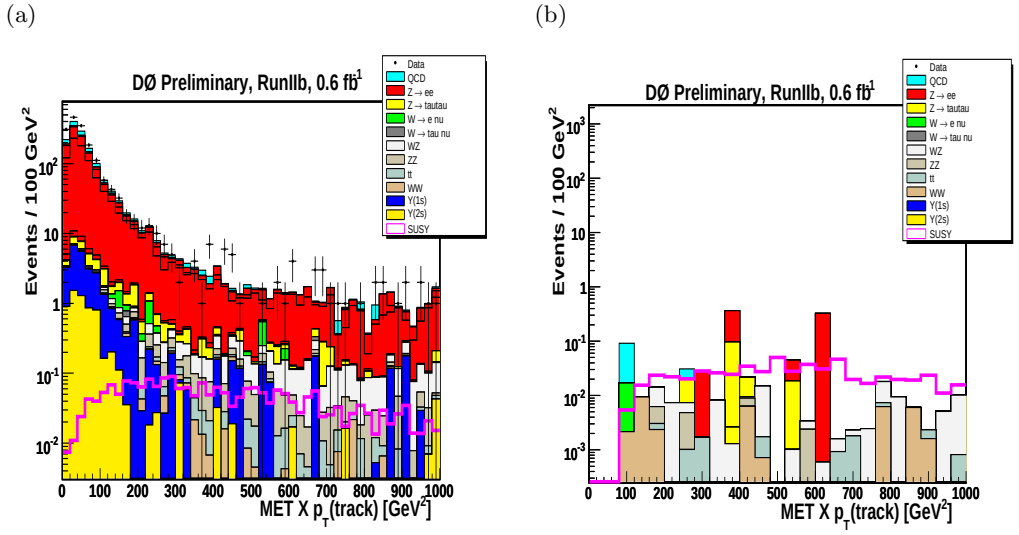

FIG. 4: Distribution of the product of $\not\!\!E_{\rm T}$ and $p_T^{\ell 3}$ (a) at preselection level in events with isolated track and (b) after $\not\!\!E_{\rm T}$ related cuts, for data (points with error bars), background simulation (histograms, complemented with the QCD expectation) and signal expectation for point LHA.131.232 [11], (empty histogram).

distribution just before the requirement of an isolated track in the event is made.

Since the LSP and the neutrinos typically cause a considerable amount of missing energy in the event, a cut on $\not\!\!E_{\rm T}$ will further reduce QCD multijet and $Z/\gamma^* \rightarrow$ ee background. Figure 2c shows the distribution for data, background and signal of the $\not\!\!E_{\rm T}$ at the preselection stage. Events with $\not\!\!E_{\rm T} < 22\,\text{GeV}$ are discarded. In addition, events are rejected if they contain jets with transverse energies above 15 GeV and have a small significance, Sig($\not\!\!E_{\rm T}$), which is defined by normalizing the $\not\!\!E_{\rm T}$ to $\sigma_{E_T^j \parallel \not\!\!E_{\rm T}}$, a measure of the jet energy resolution projected onto the $\not\!\!E_{\rm T}$ direction:

$$\mathrm{Sig}(\not\!\!E_{\mathrm{T}}) = \frac{\not\!\!E_{\mathrm{T}}}{\sqrt{\sum_{\mathrm{jets}} \sigma^2_{E_T^j \| \not\!\!E_{\mathrm{T}}}}}.$$

Figure 2d shows the distribution in data, background and signal of the $\mathrm{Sig}(\not\!\!E_{\mathrm{T}})$ at preselection level. Events with $\mathrm{Sig}(\not\!\!E_{\mathrm{T}})$ lower than 8 are discarded if there are jets in the event.

To reduce background with large $\not\!\!E_{\mathrm{T}}$ due to a poorly measured electron energy, the transverse mass of both electrons and the $\not\!\!E_{\mathrm{T}}$ is calculated. Transverse mass is defined as follows:

$$\mathrm{M_T} = \sqrt{2 \cdot \not\!\!E_{\mathrm{T}} \cdot p^l_{\mathrm{T}} \cdot (1 - \cos(\Delta\phi))}.$$

$\Delta\phi$ is the angle between the lepton and the $\not\!\!E_{\mathrm{T}}$ in the transverse plane. Events with a minimum electron-$\not\!\!E_{\mathrm{T}}$ transverse mass below 20 GeV are discarded. Figure 3 shows the minimum transverse mass distribution at preselection level.

At this stage, a large fraction of the remaining background consists of W production, where both the second electron and the third track originate from jets. To suppress this particular background component, a tightened cut on the p_T on the third track is applied if the transverse mass between the leading electron and $\not\!\!E_{\mathrm{T}}$ is compatible with the W mass. If $M_T > 65$ GeV, the p_T of the isolated track is required to be greater than 7 GeV. To further reduce $\mathrm{Z}/\gamma^* \rightarrow$ ee background where one electron is lost, the invariant mass between the isolated track and the leading electron was calculated. In such events, the lost electron is reconstructed as the third track and the second electron is a fake. If the invariant mass is between 60 GeV and 120 GeV and the track is out of the acceptance of electromagnetic calorimeter, the event is discarded. Remaining $\mathrm{Z}/\gamma^* \rightarrow$ ee and QCD multijet events are expected to have both low values of $\not\!\!E_{\mathrm{T}}$ and $p_T^{\ell 3}$. Figure 4 shows the distribution in $\not\!\!E_{\mathrm{T}} \times \mathrm{p}_{\mathrm{T}}^{\ell 3}$ for data, background and signal at preselection level in events with an isolated track (left) and after $\not\!\!E_{\mathrm{T}}$ related cuts to the right. The product of $\not\!\!E_{\mathrm{T}}$ and $\mathrm{p}_{\mathrm{T}}^{\ell 3}$ is required to be larger than 220 $(\mathrm{GeV})^2$.

IV. SYSTEMATIC UNCERTAINTIES

The estimates for expected numbers of background and signal events depend on numerous measurements that each introduce a systematic uncertainty: lepton identification, trigger efficiencies and reconstruction efficiencies (4%), trigger turn on (4-7%), jet energy scale calibration in signal ($< 1\%$) and background events (1%), lepton and track momentum calibration (1%), Parton Distribution Function (PDF) uncertainties ($< 4\%$), and modeling of multijet background (30%). The systematic error on the luminosity is mainly a combination of the PDF uncertainty (4%), uncertainty for the NNLO Z cross section (4%) and data/MC normalization factor (2%). For the estimate of the background remaining after all cuts, the systematic uncertainties are small compared to the statistical uncertainty due to limited Monte Carlo statistics. See Table III for the different sources of systematic uncertainties.

Source	Background	Signal
Electron ID, trigger, reconstruction	4%	4%
Smearing	1%	5%
QCD scale factor	1 %	-
Jet Energy Scale	$< 1\%$	$< 1\%$
WW cross sect (PDF)	1 %	-
WZ cross sect (PDF)	1 %	-
WZ backgr	10%	-
Track Momentum	1 %	1%
Trigger modeling	$4 - 7\%$	1%
Quadratic sum	12.1 %	6.6 %
Luminosity (total)	6 %	6 %
Quadratic sum total	13.5%	8.4 %

TABLE III: Systematic uncertainties on the number of events expected from Standard Model processes and from SUSY processes after the last selection cut.

TABLE IV: Number of candidate events observed and background events expected at different stages of the selection. Errors are statistical. The systematic error on background is 14.6%.

Cut	Data	Sum BG	$Z/\gamma^* \to ee$	W$\to$eν	$Z/\gamma^* \to \tau\tau$	WW/WZ	WZ	QCD multijet	$t\bar{t} \to ee$
(1) Presel	64877	65393 ± 104	59350	274	558	71	38	4157	22
(2) Anti-Z	5577	6566 ± 36	5714	61	115	14	2.4	1222	5.9
(3) Isolated Track	182	208 ± 7	173	0.01	4.7	0.26	0.60	29	0.08
(4) $\not\!\!E_{\rm T}$ related	1	1.5 ± 0.4	0.78	0.01	0.14	0.11	0.33	0.08	0.06
(5) Tr$\times\not\!\!E_{\rm T}$	0	1.0 ± 0.3	0.59	0.0	0.14	0.06	0.21	0.01	0.03

TABLE V: Number of signal events expected at different stages of the selection. For the final cut, also the signal efficiency is presented. Efficiencies are normalized to lepton events with all flavour combinations.

Cut	LHA.244.324	LHA.131.232	LHA.87.194
(1) Presel	2.9	9.0	14.1
(2) Anti-Z	1.7	5.3	8.9
(3) Isolated track	0.93	2.9	4.6
(4) $\not\!\!E_{\rm T}$ related	0.67	1.9	2.9
(5) Tr$\times\not\!\!E_{\rm T}$	0.51 ± 0.03	1.4 ± 0.1	2.1 ± 0.2
efficiency (3ℓ) [%]	3.16	2.64	2.41

V. RESULTS

The numbers of observed candidates and background events expected after application of the successive selections are listed in Table IV. The selected data and background events are in agreement and no data candidate is selected. The background expectation is $1.0 \pm 0.30 \pm 0.14$ events, dominated by Drell-Yan and di-boson events. Table V shows the number of signal events expected at different stages of the cutflow for the three signal points discussed in this analysis. The number of signal events is in the range of 0.5-2.1 events in the final selection for the three reference points mentioned in this note. Since no evidence for associated production of charginos and neutralinos is observed, an upper limit on the product of cross section and leptonic branching fraction $\sigma \times \mathrm{BR}(3\ell)$ is extracted from this result. The result of this analysis is combined with the results of $ee\ell$ [13] and $\mu^{\pm}\mu^{\pm}$ [14] from summer 2006 and with $\mu\mu\ell$ and $e\mu\ell$ from winter 2007 [15] using the modified frequentist approach [16]. The fraction of signal events that is selected by more than one selection is assigned to the selection with the largest signal-to-backround ratio and removed from all others. The expected and observed limits are shown in Figure 5 as a function of $\tilde{\chi}_1^{\pm}$mass. This result improves significantly the upper limit of about 0.2 pb presented in [5]. The cross section limit set in this analysis corresponds to a chargino mass limit of 145 GeV in the 3ℓ-max scenario. Assuming the mSUGRA-inspired mass relation $m_{\tilde{\chi}_1^{\pm}} \approx m_{\tilde{\chi}_2^0} \approx 2m_{\tilde{\chi}_1^0}$ as well as degenerate slepton masses $m_{\tilde{\ell}}$ (no slepton mixing), the limit on $\sigma \times \mathrm{BR}(3\ell)$ is a function of $m_{\tilde{\chi}_1^{\pm}}$ and $m_{\tilde{\ell}}$ with a relatively small dependence of the other SUSY parameters. This result can therefore be interpreted in more general SUSY scenarios as long as the above mass relations are satisfied and $R-$ parity is conserved. The leptonic branching fraction of chargino and neutralino depends on the relative contribution from the slepton- and W/Z-exchange graphs, which varies as a function of the slepton masses. W/Z exchange is dominant at large slepton masses, resulting in relatively small leptonic branching fractions (large m_0 scenario). The leptonic branching fraction for three-body decays is maximally enhanced for $m_{\tilde{\ell}} \gtrsim m_{\tilde{\chi}_2^0}$ (3ℓ-max scenario). Decays into leptons can even be dominant if sleptons are light enough that two-body decays are possible. In the latter case, one of the leptons from the neutralino decay can have a very low transverse momentum if the mass difference beween neutralino and sleptons is small. In this region, only the $\mu^{\pm}\mu^{\pm}$ selection remains efficient, leading to a slightly higher limit for -6 $\lesssim m_{\tilde{\ell}} - m_{\tilde{\chi}_2^0} \leq 0$ (see Fig. 6). In addition, the $\tilde{\chi}_1^{\pm}\tilde{\chi}_2^0$ production cross section depends on the squark masses due to the negative interference with the t-channel squark exchange. Relaxing scalar mass unification, the cross section is maximal in the limit of large squark masses (heavy-squarks scenario).

VI. CONCLUSIONS

A search has been performed for the trilepton decay signature from the associated production of the lightest chargino and the next-to-lightest neutralino in leptonic channels with two electrons, using data corresponding to an integrated

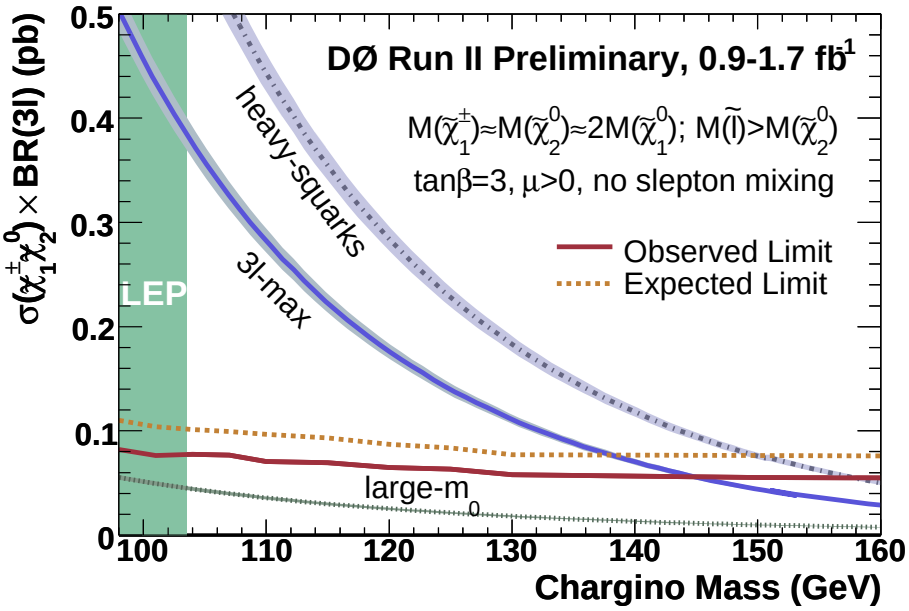

FIG. 5: Limit on $\sigma \times \mathrm{BR}(3\ell)$ as a function of $\tilde{\chi}_1^{\pm}$ mass, in comparison with the expectation for several SUSY scenarios. The red line corresponds to observed mSUGRA limit. PDF and renormalization/factorization scale uncertainties are shown as shaded bands.

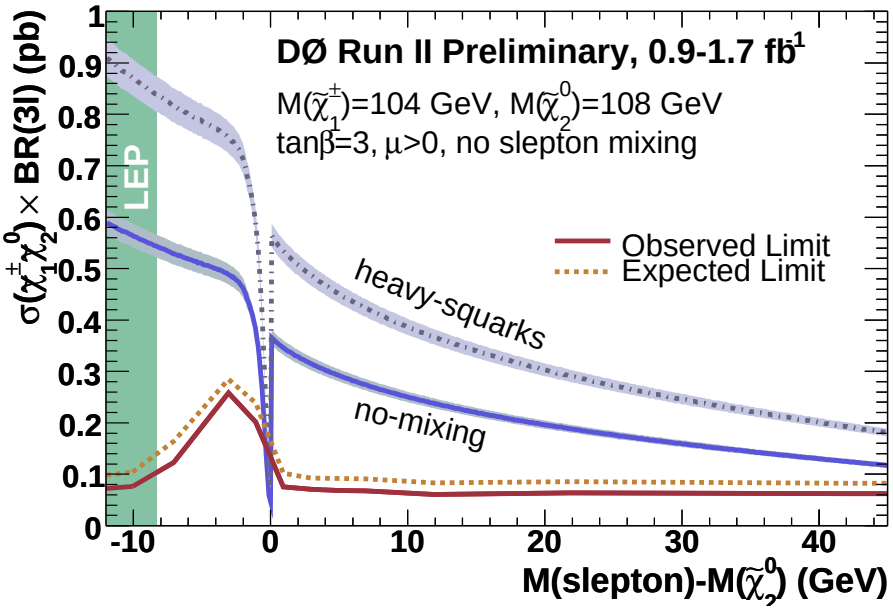

FIG. 6: Limit on $\sigma \times \mathrm{BR}(3\ell)$ as a function of the mass difference between sleptons and $\tilde{\chi}_2^0$, in comparison with the expectation for the MSSM (no mixing) and the heavy-squarks scenario (see text). PDF and renormalization/factorization scale uncertainties are shown as shaded bands. $\mathrm{BR}(3\ell)$ drops at $m_{\tilde{\ell}} \lesssim m_{\tilde{\chi}_2^0}$ as the phase space for two body decays into real sleptons is minimal.

luminosity of around 590 pb^{-1}. No evidence for supersymmetry is observed and upper limits on the product of cross section and leptonic branching fraction are set, representing an improvement upon previous limits set. Chargino mass limits beyond the reach of LEP chargino searches are derived for several SUSY reference scenarios with enhanced leptonic branching fractions.

Acknowledgments

We thank the staffs at Fermilab and collaborating institutions, and acknowledge support from the Department of Energy and National Science Foundation (USA), Commissariat à l'Energie Atomique and CNRS/Institut National de Physique Nucléaire et de Physique des Particules (France), Ministry of Education and Science, Agency for Atomic Energy and RF President Grants Program (Russia), CAPES, CNPq, FAPERJ, FAPESP and FUNDUNESP (Brazil), Departments of Atomic Energy and Science and Technology (India), Colciencias (Colombia), CONACyT (Mexico), KRF (Korea), CONICET and UBACyT (Argentina), The Foundation for Fundamental Research on Matter (The Netherlands), PPARC (United Kingdom), Ministry of Education (Czech Republic), Natural Sciences and Engineering Research Council and WestGrid Project (Canada), BMBF (Germany), A.P. Sloan Foundation, Civilian Research and Development Foundation, Research Corporation, Texas Advanced Research Program, and the Alexander von Humboldt Foundation.

---

[1] H.P. Nilles, Phys. Rep. **110** (1984) 1;
H.E. Haber and G.L. Kane, Phys. Rep. **117** (1985) 75.
[2] W.Beenakker *et al., The production of Charginos/Neutralinos and Sleptons at Hadron Colliders*, hep-ph/9906298.
[3] LEPSUSYWG, ALEPH, DELPHI, L3 and OPAL experiments,
note LEPSUSYWG/01-07.1, (`http://lepsusy.web.cern.ch/lepsusy /Welcome.html`)
[4] B.Abbott *et al.,* (DØ Collaboration), Phys. Rev. Lett. **80** (1998) 8.
[5] V. Abazov *et al.,* (DØ Collaboration), *Search for supersymmetry via associated production of charginos and neutralinos in final states with three leptons*, Phys. Rev. Lett. **95** (2005) 8.
[6] F. Abe *et al.,* (CDF Collaboration), *Search for Chargino-Neutralino Associated Production at the Fermilab Tevatron Collider*, Phys. Rev. Lett. **80**, 5275 (1998).
[7] V. Abazov *et al.,* (DØ Collaboration), *The Upgraded DØ Detector*, Nucl. Instrum. Meth. A **565**, 463 (2006), FERMILAB-PUB-05-341-E (2005).
[8] R. Hamberg, W.L. van Neerven, and T. Matsuura, Nucl. Phys. **B359**, 343 (1991) [Erratum-ibid. **B644**, 403 (2002)].
[9] T. Nunnemann, DØ Note 4476.
[10] T. Sjostrand, Comp. Phys. Commun. **82** (1994) 74, `CERN-TH 7112/93` (1993).
[11] P. Skands *et al.,* JHEP 07, 036 (2004).
[12] J. Kozminski, R. Kehoe, H. Weerts, S. Park, A. Quadt, J. Gardner, Sh. Jabeen, *'Electron Likelihood in p14'*, DØ Note 4449.
[13] V. Abazov *et al.,* (DØ Collaboration), *Search for the Associated Production of Chargino and Neutralino in Final States with Two Electrons and an Additional Lepton*, DØ Note 5131. (`http://www-d0.fnal.gov/Run2Physics/WWW/results/prelim/NP/N46/`).
[14] V. Lesne, *Search for the associated production of charginos and neutralinos in like sign dimuon channel*, DØ Note 5126. (`http://www-d0.fnal.gov/Run2Physics/WWW/results/prelim/NP/N45/`).
[15] V. Abazov *et al.,* (DØ Collaboration), *Search for the Associated Production of Chargino and Neutralino in Final States with Three Leptons*, DØ Note 5348. (`http://www-d0.fnal.gov/Run2Physics/WWW/results/prelim/NP/N52/`).
[16] T. Junk, Nucl. Instr. and Meth., A**434** (1999) 435.